Reprinted from the *Soil Science Society of America Journal*
Volume GO, no. 1, January-February 1996
677 South Segoe **Rd., Madison, WI 5371** l USA

Modeling Competitive Adsorption of Arsenate with Phosphate and Molybdate on Oxide Minerals

Bruce A. Manning* and S. Goldberg

ABSTRACT

The mobility of As in **soils depends on several factors including redox potential, soil mineralogy, pH, and the presence of other oxyanions that compete with As for soil retention sites. We investigated the effects of pH and competing anions on the adsorption of arsenate [As(V)] on a-FeOOH (goethite) and γ-Al(OH)$_3$ (gibbsite). Batch equilibrium As(V) adsorption experiments were conducted with P and Mo as competing anions in order to produce single-anion [As(V), P, and Mo] and binary-anion [As(V/P and As(V)/Mo] adsorption envelopes (adsorption vs. solution pH). Arsenate and P single-anion adsorption envelopes were similar with substantial adsorption occurring across a wide pH range, including pH values above the points of zero charge of the oxides. Maximum Mo adsorption occurred across a narrower pH range (pH 4-6). On both oxides, equimolar P concentrations decreased As(V) adsorption within the pH range 2 to 11, whereas Mo decreased As(V) adsorption only below pH 6. The constant capacitance model was used to predict competitive surface complexation behavior between As(V)/P and As(V)/Mo using intrinsic equilibrium constants [K_{anion} tint)] optimized from single-anion data. In addition, the model was applied using one-site (monodentate) and two-site (monodentate + bidentate) conceptualizations of the oxide surface. The two approaches gave comparable fits to experimental adsorption data and were consistent with competitive adsorption observed in binary adsorption envelopes.**

THE REACTIVITY of As(V) with individual soil minerals is important in determining the general mobility of As in whole soils. Arsenate is the predominant inorganic species of As under oxidizing soil conditions (Sadiq et al., 1983; Masscheleyn et al., 1991) and is retained in soils by adsorption reactions (Roy et al., 1986; Goldberg and Glaubig, 1988). Important minerals that control the As(V) adsorption capacity of soils include Fe and Al oxides (Jacobs et al., 1970; Livesey and Huang, 1981; Fuller et al., 1993). Investigations of As(V) adsorption on Fe and Al oxides have generated considerable evidence for the formation of inner-sphere As(V) surface complexes (Hingston et al., 1971; Anderson and Malotky, 1979). Direct spectroscopic evidence for inner-sphere adsorption of As(V) on Fe oxide has been obtained using EXAFS (Waychunas et al., 1993), energy dispersive analysis of x-rays (EDAX) (Hsia et al., 1994), and infrared spectroscopy (Harrison and Berkheiser, 1982; Lumsdon et al., 1984).

Arsenate, phosphate, and molybdate are tetrahedral oxyanions (Cotton and Wilkinson, 1980) that can compete for adsorption sites on soil mineral surfaces (Murali and Aylmore, 1983). Hingston (198 1) estimated the mean areas occupied by the AsO_4, PO_4, and MoO_4 tetrahedra on the goethite surface to be 0.61, 0.61, and 0.31 nm^2, respectively. Competitive adsorption between As(V), P, and Mo has been described in whole soils with a competitive Freundlich-type isotherm equation (Roy et al., 1986), though the applicability of the model was limited to cases where the As/P and As/Mo equilibrium concentration ratios were >20. Barrow (1974) investigated As(V) and P competitive adsorption in soil and found that, though As(V) desorbed some previously adsorbed P, a substantial portion of the bound P was not displaced by As(V). Based on competitive adsorption between As(V) and P on goethite, Hingston et al. (1971) postulated that the goethite surface contains adsorption sites common to both As(V) and P anions, as well as sites that adsorb either one anion or the other. The ability to predict As(V) adsorption in complicated systems such as whole soils will require quantitative information on the adsorption of As(V) by individual soil minerals in the presence of competing anions.

Though several studies have investigated As(V) adsorption on oxide minerals (e.g., Hingston et al., 1971; Anderson and Malotky , 1979; Leckie et al., 1980; Pierce and Moore, 1982), only a few studies (e.g., Goldberg, 1986; Belzile and Tessier, 1990) have investigated surface complexation modeling as a means of quantifying the surface reactions of As(V). The CCM of the oxide-water interface (Schindler and Gamsjäger, 1972; Hohl and Stumm, 1976; Schindler et al., 1976; Stumm et al., 1976, 1980) has been used to investigate As(V) adsorption on soil materials (Goldberg, 1986; Goldberg and Glaubig, 1988). Good agreement has been found between binding constants for As(V) adsorption on amorphous Fe oxyhydroxide derived from field data and those obtained in the laboratory (Belzile and Tessier, 1990).

The objectives of this study were to investigate the ability of the CCM to predict As(V) competitive adsorption on goethite and gibbsite and to evaluate the ability of the model to describe oxyanion adsorption using both mono- and bidentate surface complexes. Experimental single-anion [As(V), P, and Mo] adsorption envelopes were generated in the laboratory and used for optimizing intrinsic equilibrium constants. The set of constants that were optimized in single-anion systems were then used as fixed parameters to predict competitive adsorption in a separate set of binary As(V)/P and As(V)/Mo experimental adsorption data.

MATERIALS AND METHODS

Synthetic Oxides

Synthetic goethite was prepared by the method of McLaughlin et al. (1981). The pH of a 0.2 *M* $Fe(NO_3)_3$ solution was adjusted to 11 .0 with 0.2 *M* NaOH and the suspension stored

USDA-ARS, U.S. Salinity Lab., 450 West Big Springs Road, Riverside, CA 92507-4617. Contribution from the U. S. Salinity Lab. Received 6 Feb. 1995. *Corresponding author.

Published in Soil Sci. Soc. Am. J. 60:121-131 (1996).

Abbreviations: EXAFS, extended x-ray absorption fine structure; EDAX, energy dispersive analysis of x-rays; CCM; constant capacitance model; DI, deionized; BET, Brtmauer-Emmett-Teller; EM, electrophoretic mobility; PZC, point of zero charge; IC, ion chromatography.

at room temperature (22 ± 1 "C) for 2 d. The suspension was then heated in a water bath at 90°C for 16 h followed by repeated rinsing of the solids with deionized (DI) water. Gibbsite was prepared according to the procedure of Kyle et al. (1975) by slowly adding 4 M NaOH to 1 M $AlCl_3$ while stirring until the pH stabilized at 4.6. After heating in a water bath at 40°C for 2 h, the precipitate was transferred to cellulose tubing and dialyzed with DI water for 36 d. Goethite and gibbsite solids were dried overnight in a gravity convection oven at 70 and 40°C, respectively. The solids were ground with a mortar and pestle to pass a 500-μm sieve and the identity of the oxides was confirmed by x-ray diffraction analysis of random powder mounts. The specific surface areas of the oxides were determined by single-point BET N_2 adsorption with a Quantisorb Jr. flow-through surface area analyzer (Quantachrome Corp., Syosset, NY).

Electrophoretic Mobility

The EM of oxide particles was determined with a Zeta-Meter System 3.0 (Zeta-Meter, Long Island City, NY) equipped with a microscope module and flow-through sample transfer system. A suspension containing 50 mg solid in 500 mL of 0.001 *M* HCl was equilibrated 1 h and the average EM of at least 20 particles was recorded at each pH by titrating the stirred suspension with 0.001 *M* NaOH. The EM of goethite and gibbsite particles was also measured in the presence and absence of 133 μ*M* As(V) using the same method. The PZC of the oxides were estimated from plots of EM as a function of pH by interpolation to zero EM (Hunter, 1981).

Arsenate, Phosphate, and Molybdate Adsorption Envelopes

Anion adsorption envelopes were produced using batch reactions in 40-mL polycarbonate centrifuge tubes. Stock solutions of As(V), P, and Mo were prepared in 0.1 *M* NaCl from the sodium salts $Na_2AsO_4 \cdot 7H_2O$, $NaH_2PO_4 \cdot H_2O$, and $Na_2MoO_4 \cdot 2H_2O$, respectively. Twenty milliliters of 133 or 266 μ*M* As(V), P, or Mo in 0.1 *M* NaCl were added directly to 50 mg of oxide in the centrifuge tubes. Binary anion systems contained 266 μ*M* total anion concentration [133 μ*M* As(V) + 133 μ*M* P or Mo]. The pH was adjusted to range between 3 and 11 with not more than 0.5 mL of 0.1 M NaOH or HCl. The tubes were shaken for 4 h at room temperature (22 ± 1 "C) on a reciprocating shaker and centrifuged at 12 500 g for 10 min. Preliminary work verified that As(V) adsorption had stabilized after 4 h and no further reaction time was required. Supematant pH was measured with a Thomas glass combination pH electrode (Thomas Scientific, Swedesboro, NJ) and a Beckman potentiometer (Beckman Instruments, Fullerton, CA) followed by filtering with 0. 1-μm pore size Whatman cellulose nitrate membrane filters. The amount of anion adsorbed was calculated as the difference between the anion concentration before and after reaction with the solids.

Anion concentrations were determined using a Dionex 2000 ion chromatograph (Dionex Corp., Sunnyvale, CA) with an OmniPac PAX-500 column (4.6 by 250 mm), an eluent (15 mM NaOH) flow rate of 0.75 mL min^{-1}, and suppressed ion conductivity detection. Peak areas were measured with a Hewlett Packard 3390 reporting integrator. Average analyte retention times were 6.0, 6.9, and 9.5 min for Mo, P, and As(V), respectively. The As(V), Mo, and P detection limits of the technique were approximately 1.0 to 1.2 μ*M* with typically better than 5% precision in the peak area measurement. Prior to IC analyses, Cl- was removed from sample solutions with Dionex On-guard Ag solid-phase extraction columns (7 by 5 mm i.d.). Fifteen milliliters of DI water and then 5 mL of sample were forced through the columns with a syringe and discarded, followed by 10 mL of sample, which was saved for IC analysis.

The Constant Capacitance Model

The CCM was used to predict As(V), P, and Mo adsorption in binary anion systems. This model is based on the following assumptions: (i) ion adsorption occurs by an inner-sphere ligand exchange mechanism, (ii) no complexes are formed with ions of the background electrolyte, and (iii) the net surface charge, σ_o (mol$_c$ L^{-1}), is a linear function of the surface potential, ψ_o (volts):

$$\sigma_o = (CS_A M_V/F)\psi_o \quad [1]$$

where subscript o refers to the surface, C (F m^{-2}) is the capacitance density at the surface, S_A (m^2 g^{-1}) is the specific surface area, M_V (*g* L^{-1}) is the suspension density of the solid, and *F* (9.65 x 10^{-4} coulombs mol^{-1}) is the Faraday constant. The capacitance density, C, was fixed at 1.06 F m^{-2} (Westall and Hohl, 1980).

The CCM uses the following set of reactions to calculate monodentate specific adsorption of As(V) on the oxide surface:

$$SOH + H^+ \rightleftarrows SOH_2^+ \quad [2]$$

$$SOH \rightleftarrows SO^- + H^+ \quad [3]$$

$$SOH + H_3AsO_4 \rightleftarrows SH_2AsO_4 + H_2O \quad [4]$$

$$SOH + H_3AsO_4 \rightleftarrows SHAsO_4^- + H_2O + H^+ \quad [5]$$

$$SOH + H_3AsO_4 \rightleftarrows SAsO_4^{2-} + H_2O + 2H^+ \quad [6]$$

where SOH is defined as 1 mol of reactive hydroxyl groups on the oxide surface. An identical set of P adsorption reactions could be written by replacing As with P in Eq. [4] through [6]. The surface reactions in Eq. [4] through [6] are written using the model *components* as reactants to form model surface *species* as products. Components are the fundamental entities from which all species can be derived. The model components used for As(V) single-anion monodentate systems were SOH, H_3AsO_4, H^+, and ψ_o. Equations [4] through [6] do not represent the actual reactions that occur at the surface, but are written so as to form species (e.g., SOH_2^+, $SAsO_4^{2-}$, etc.) only from components. The analogous set of reactions for Mo are:

$$SOH + H_2MoO_4 \rightleftarrows SHMoO_4 + H_2O \quad [7]$$

$$SOH + H_2MoO_4 \rightleftarrows SMoO_4^- + H_2O + H^+ \quad [8]$$

The CCM uses intrinsic equilibrium constants, which account for surface charge produced by reactions [2] through [8]:

$$K_{S+}(\text{int}) = \frac{[SOH_2^+]}{[SOH][H^+]} \exp(F\psi_o/RT) \quad [9]$$

$$K_{S-}(\text{int}) = \frac{[SO^-][H^+]}{[SOH]} \exp(-F\psi_o/RT) \quad [10]$$

$$K^1_{SAs}(\text{int}) = \frac{[SH_2AsO_4]}{[SOH][H_3AsO_4]} \quad [11]$$

$$K^2_{SAs}(\text{int}) = \frac{[SAsO_4^{2-}][H^+]^2}{[SOH][H_3AsO_4]} \exp(-2F\psi_o/RT) \quad [12]$$

$$K^3_{SAs}(\text{int}) = \frac{[SAsO_4^{2-}][H^+]^2}{[SOH][H_3AsO_4]} \exp(-2F\psi_o/RT) \quad [13]$$

where *R* is the molar universal gas constant, T is the absolute temperature (K), and brackets refer to concentrations (mol

L^{-1}). Again, the analogous set of intrinsic equilibrium constants for the P surface complexes could be described by replacing As with P in Eq. [1 l] through [13]. The intrinsic equilibrium constants for the two molybdate surface complexes in Eq. [7] and [8] are

$$K^1_{SMo}(\text{int}) = \frac{[SHMoO_4]}{[SOH][H_2MoO_4]} \quad [14]$$

$$K^2_{SMo}(\text{int}) = \frac{[SMoO_4^-][H^+]}{[SOH][H_2MoO_4]} \exp(-F\psi_o/RT) \quad [15]$$

Mass and charge balance expressions for surface functional groups are contained in the CCM and take the following forms for the case of single As(V) anion adsorption:

$$[SOH]_T = [SOH] + [SOH_2^+] + [SO\text{-}] + [SH_2AsO_4] + [SHAsO_4^-] + [SAsO_4^{2-}] \quad [16]$$

$$\sigma_o = [SOH_2^+] - [SO\text{-}] - [SHAsO_4^-] - 2[SAsO_4^{2-}] \quad [17]$$

For the case of binary As(V) and P adsorption, Eq. [16] and [17] take the form

$$[SOH]_T = [SOH] + [SOH_2^+] + [SO\text{-}] + [SH_2AsO_4] + [SHAsO_4^-] + [SAsO_4^{2-}] + [SH_2PO_4] + [SHPO_4^-] + [SPO_4^{2-}] \quad [18]$$

and

$$\sigma_o = [SOH_2^+] - [SO\text{-}] - [SHAsO_4^-] - 2[SAsO_4^{2-}] - [SHPO_4^-] - 2[SPO_4^{2-}] \quad [19]$$

The computer program FITEQL Version 3.1 (Herbelin and Westall, 1994) is an iterative nonlinear least squares optimization routine, which was used to fit intrinsic equilibrium constants of the CCM (e.g., Eq. [1 1]-[13]) to experimental As(V), P, and Mo adsorption data. FITEQL contains a choice of four adsorption models: constant capacitance, diffuse layer, Stern, and triple layer. More detailed discussions on using FITEQL are given elsewhere (Westall, 1982; Goldberg, 1995).

The FITEQL program was used in two different modes to fit the CCM to the experimental data: (i) optimization of the set of single-anion $K_{anion}(\text{int})$ values using the least squares optimization routine, and (ii) bypassing the optimization routine and fitting the set of single-anion $K_{anion}(\text{int})$ values by visual inspection of model output. After optimization, experimental binary adsorption data were predicted without adjustable parameters using $K_{anion}(\text{int})$ values that were derived from single-anion systems. A goodness of fit parameter is included in the the FITEQL output when the least squares optimization procedure is used; however, because some data were optimized visually it was not used to judge or compare the quality of the model fits.

Various physical and chemical properties of the solid adsorbent material are required before surface complexation modeling can be applied to experimental adsorption data. These values are generally chosen as fixed parameters and include surface area, the reactive surface site density (N_d, mol m^{-2}), and the protonation and deprotonation reaction constants [$K_{\pm}(\text{int})$] for the surface hydroxyl functional group (Eq. [2] and [3]). The total number of surface sites in a suspension (N_s, mol L^{-1}) was calculated using the following expression

$$N_s = N_d S_A M_V \quad [20]$$

where N_d (sites m^{-2}) is the surface site density for the sorbent.

Table 1. Numerical input values and intrinsic equilibrium constants optimized in single-anion As(V), **P, and** Mo systems using the constant capacitance model with the one-site (SOH) assumption.

	Goethite	Gibbsite
Surface area (S_A), $m^2\ g^{-1}$	43.1	45.0
Total sites (Iv'.), x 10^{-4} mol L^{-1}	4.19	4.32
$\log K_{S+}(\text{int})$†	7.52	9.10
$\log K_{S-}(\text{int})$	− 10.6	− 10.5
$\log K^1_{SAs}(\text{int})$	8.40	8.60
$\log K^2_{SAs}(\text{int})$	3.40	2.20
$\log K^3_{SAs}(\text{int})$	− 2.30	− 5.70
$\log K^1_{SP}(\text{int})$	8.05	9.90
$\log K^2_{SP}(\text{int})$	3.40	3.20
$\log K^3_{SP}(\text{int})$	− 2.20	− 4.70
$\log K^1_{SMo}(\text{int})$	7.90	7.54
$\log K^2_{SMo}(\text{int})$	1.70	0.30
Capacitance density, F m^{-2}	1.06	
Suspension density, g L^{-1}	2.5	
Background electrolyte	0.1 M NaCl	

† Intrinsic equilibrium constants were calculated as mol L^{-1}.

The N_d value of 2.31 sites nm^{-2} (3.84 x 10^{-6} mol sites m^{-2}) (Davis and Kent, 1990) was used for both oxides and calculated N_s values were 4.19 x 10^{-4} and 4.32 x 10^{-4} mol sites L^{-1} for goethite and gibbsite, respectively (see Table 1). In addition to surface properties, acidity constants for the adsorbing anions (K_a values), which are readily available in the literature (e.g., Lindsay, 1979; Dzombak and Morel, 1990), are also required prior to model application.

Values of $K_{S\pm}(\text{int})$ for modeling oxide surface reactions can either be obtained experimentally from potentiometric data, used as adjustable parameters, or taken from the literature. In the one-site (monodentate only) approach used in this study (see below), established $K_{S\pm}(\text{int})$ values for goethite (Lumsdon and Evans, 1994) were used. For gibbsite, values of $K_{S\pm}(\text{int})$ for the one-site approach were used as adjustable parameters but were constrained to agree with the PZC as measured by electrophoretic mobility according to the equation

$$\text{PZC} = 0.5[|\log K_+(\text{int})| + |\log K_-(\text{int})|] \quad [21]$$

The two-site (monodentate + bidentate) modeling approach (also, see below) required both $K_{S\pm}(\text{int})$ and $K_{X\pm}(\text{int})$ values and are given in Table 2.

Table 2. Intrinsic equilibrium constants optimized in single-anion As(V), P, and Mo systems using the constant capacitance model with the two-site [$X(OH)_2$ + SOH] assumption.7

	Goethite	Gibbsite
Total sites (N_s), x 10^{-4} mol L^{-1}	4.19	4.32
Bidentate site [$X(OH)_2$]		
$N_{X(OH2}$, x 10^{-4} mol L^{-1}	2.19	2.32
$\log K_{X+}(\text{int})$‡	1.52	9.10
$\log K_{X-}(\text{int})$	− 10.6	− 10.5
$\log K^1_{XAs}(\text{int})$	8.90	1.75
$\log K^2_{XAs}(\text{int})$	2.90	2.90
$\log K^1_{XP}(\text{int})$	8.90	9.90
$\log K^2_{XP}(\text{int})$	3.10	3.20
$\log K^1_{XMo}(\text{int})$	8.50	9.10
Monodentate site (SOH)		
N_{SOH} (x 10^{-4} mol L^{-1})	2.00	2.00
$\log K_{S+}(\text{int})$	11.0	10.0
$\log_{S-}(\text{int})$	− 13.0	− 12.0
$\log K^1_{SAs}(\text{int})$	− 2.40	− 5.70
$\log K^1_{SP}(\text{int})$	− 2.30	− 4.70
$\log K^1_{SMo}(\text{int})$	3.10	0.90

† Input values (e.g., S_A and M_V) used to predict competitive adsorption other than intrinsic equilibrium constants are given in Table 1.
‡ Intrinsic equilibrium constants were calculated as mol L^{-1}.

We have attempted to incorporate recent evidence for the formation of both mono- and bidentate As(V) surface complexes on FeOOH polymorphs such as goethite (Waychunas et al., 1993). Based on EXAFS spectra, Waychunas et al. (1993) reported that As(V) adsorption on ferrihydrite at pH 8 resulted in approximately 30% monodentate attachment, with the remainder as bidentate. Monodentate As(V) attachment was most pronounced on goethite when the As(V) surface coverage was low (5% of maximum) and decreased with increasing As(V) coverage (Waychunas et al., 1993). This information was used as a constraint when modeling monodentate + bidentate attachment of As(V).

One-Site Adsorption Modeling

The one-site model used in this study assumes that only one type of surface hydroxyl group (SOH) is involved in surface complexation reactions. We further restricted the one-site model to assume only monodentate attachment at the oxide surface, which is represented by the reactions in Eq. [4] through [6]. Bidentate ligand attachment to an oxide surface could also be included in the one-site model as (Hohl et al., 1980)

$$2SOH + H_3AsO_4 \rightleftarrows (SO)_2HAsO_4 + 2H_2O \quad [22]$$

$$2SOH + H_3AsO_4 \rightleftarrows (SO)_2AsO_4^- + 2H_2O + H^+ \quad [23]$$

In this conceptualization of the reactive surface, SOH is a hydroxyl group identical to the SOH proposed for the reactions to form the monodentate surface species in Eq. [4] through [6], which can form both mono- and bidentate surface complexes. The approach outlined in Eq. [22] and [23] was not used, however, due to difficulties encountered in modeling the formation of both mono- and bidentate complexes with SOH as the only reactive site: (i) the least-squares optimization routine in the FITEQL program would not converge on values for $K_{anion}(int)$, (ii) when the optimization routine in FITEQL was bypassed and the program used to fit experimental adsorption data by visual inspection, the overall shapes of calculated adsorption envelopes were in poor general agreement with experimental data, and (iii) the As(V) surface attachment, i.e., the partitioning of adsorbed As(V) between mono- and bidentate complexes, was in poor agreement with the data of Waychunas et al. (1993). Table 1 contains the sets of $\log K(int)$ values used in modeling experimental adsorption data with the one-site (monodentate only) assumptions.

Two-Site Adsorption Modeling

In order to incorporate bidentate ligand attachment into the CCM while at the same time providing satisfactory fits to experimental data, a two-site approach was taken where mono- and bidentate attachment were assumed to occur at two separate sites [SOH and $X(OH)_2$]. In this conceptualization of the reactive surface, the hydroxyl group at the monodentate-only site (SOH) is assumed to be topologically and geometrically distinct from the hydroxyl groups at the bidentate $X(OH)_2$ site. The two-site model required subdivision of N_s

$$N_s = N_{SOH} + N_{X(OH)2} \quad [24]$$

where N_{SOH} and $N_{X(OH)2}$ (mol L^{-1}) are the amounts of reactive monodentate and bidentate sites in the suspension, respectively. Values of N_{SOH} and $N_{X(OH)2}$ (Table 2) were chosen in order to constrain model output to be approximately 30 % monodentate As(V) coverage on goethite at pH 8. The reactions for the $X(OH)_2$ site that were used in modeling are

$$X(OH)_2 + H^+ \rightleftarrows HOXOH_2^+ \quad [25]$$

$$X(OH)_2 \rightleftarrows HOXO^- + H^+ \quad [26]$$

$$X(OH)_2 + H_3AsO_4 \rightleftarrows XHAsO_4 + 2H_2O \quad [27]$$

$$X(OH)_2 + H_3AsO_4 \rightleftarrows XAsO_4^- + 2H_2O + H^+ \quad [28]$$

Expressions for the intrinsic equilibrium constants that correspond to Eq. [25] through [28] are

$$K_{X+}(int) = \frac{[HOXOH:]}{[X(OH)_2][H^+]} \exp(F\psi_o/RT) \quad [29]$$

$$K_{X-}(int) = \frac{[HOXO^-][H^+]}{[X(OH)_2]} \exp(-F\psi_o/RT) \quad [30]$$

$$K^1_{XAs}(int) = \frac{[XHAsO_4]}{[X(OH)_2][H_3AsO_4]} \quad [31]$$

$$K^2_{XAs}(int) = \frac{[XAsO_4^-][H^+]}{[X(OH)_2][H_3AsO_4]} \exp(-F\psi_o/RT) \quad [32]$$

On the SOH site, only the fully deprotonated As(V), P, and Mo surface species (i.e., $SAsO_4^{2-}$, SPO_4^{2-}, and $SMoO_4^-$) were considered (see Eq. [6]) because it was assumed that protonation of surface hydroxyls at low pH would favor bidentate vs. monodentate bonding overall, i.e.

$$[SH_2AsO_4] + [SHAsO_4^-] + [SAsO_4^{2-}] \approx [SAsO_4^{2-}] \quad [33]$$

The primary justification for this assumption was that no spectroscopic data are available that describe the effects of pH on the distribution between mono- and bidentate As(V) attachment. The surface site mass balance expression for the two-site binary As(V)/P case is

$$N_s = [X(OH)_2]_T + [SOH]_T \quad [34]$$

where

$$[SOH]_T = [SOH] + [SOH_2^+] + [SO^-] + [SAsO_4^{2-}] + [SPO_4^{2-}] \quad [35]$$

and

$$[X(OH)_2]_T = [X(OH)_2] + [HOXOH_2^+] + [HOXO^-] + [XHAsO_4] + [XAsO_4^-] + [XHPO_4] + [XPO_4^-] \quad [36]$$

Values of $\log K_{Anion}(int)$ and $\log K_{S\pm}(int)$ used in the two-site model approach are given in Table 2.

RESULTS AND DISCUSSION

Electrophoretic Mobility

The PZC values of goethite and gibbsite measured by electrophoretic mobility with no As(V) present were 8.7 and 9.8, respectively (Fig. 1). Reported PZC values for goethite range between 7.60 and 9.38 (Lumsdon and Evans, 1994). For gibbsite , PZC values of 9.5 (Hingston et al., 1972) and 9.6 (Goldberg et al., 1993) have been reported. We did not measure As(V) adsorption during the EM titration, though it is clear that As(V) adsorption decreased the PZC values of goethite to 2.8 (-5.8 pH units) and that of gibbsite to 5.8 (-4.0 pH units). A decrease in PZC resulting from an adsorption reaction is macroscopic evidence for inner-sphere specific anion

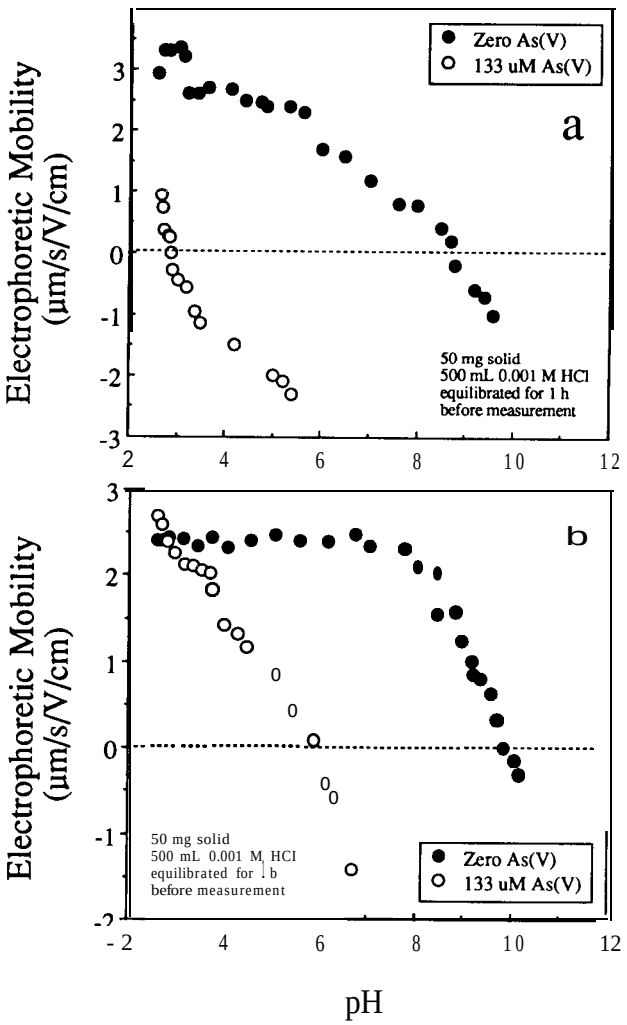

Fig. 1. Electrophoretic mobility of goethite (α-FeOOH) (a) and gibbsite [γ-Al(OH)$_3$] (b) in the presence and absence of adsorbed As(V). Points of zero charge (PZC) of the oxides were estimated from the pH of zero electrophoretic mobility.

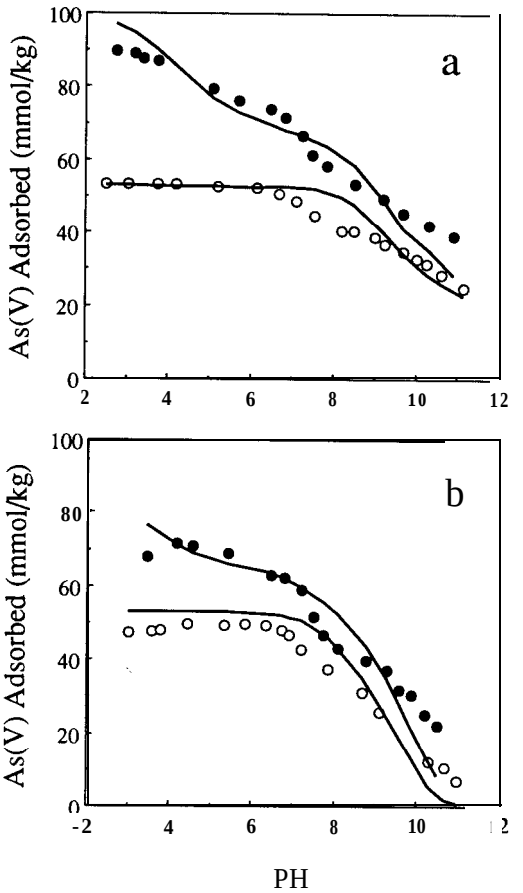

Fig. 2. Arsenate adsorption envelopes on (a) goethite (α-FeOOH) and (b) gibbsite [γ-Al(OH)$_3$] at two As(V) loadings. Constant capacitance model calculations using the one-site (SOH) assumption (lines) rep resent the sum of As(V) surface species as calculated by the model. Reaction conditions: 266 µ*M* As(V) (filled circles) or 133 µ*M* As(V) (open circles), 0.1 M NaCl, 2.5 g L^{-1} solid, reaction time = 4 h, *T* = 23°C.

adsorption (Hunter, 198 1) caused by an increase in negative surface charge. Other investigations of anion adsorption on Fe and Al oxides (Hingston et al., 1972; Anderson and Malotky, 1979; Ferreiro et al., 1985; Zhang and Sparks, 1989; Waychunas et al., 1993; Hsia et al., 1994) indicate that As(V), P, and Mo are adsorbed by an inner-sphere mechanism. Specific adsorption of protolyzable anions on oxide surfaces provides new surface acidity functional groups (Anderson and Malotky, 1979), which undergo protonation reactions. The large increase in negative surface charge resulting from As(V) adsorption suggests that the As(V) surface species may be deprotonated as in Eq. [5], [6], and [28]. This is consistent with the assumption in the two-site modeling approach stated in Eq. [33], which emphasizes the importance of the negatively charged surface species.

One-Site Adsorption Modeling

Arsenate adsorption envelopes on goethite and gibbsite at two As(V) concentrations [133 and 266 µ*M* As(V)] are shown in Fig. 2 along with CCM results using the one-site assumption. At the 266 µ*M* As(V) starting concentration, As(V) surface coverages reached a maximum of 90 mmol As(V) kg-' on goethite at pH 3.0 (Fig. 2a) and 73 mmol As(V) kg-' on gibbsite at pH 4.3 (Fig. 2b). These As(V) surface coverages were 54% (goethite) and 42% (gibbsite) of the total number of binding sites (SOH) used in the model. At the 133 µ*M* As(V) starting concentration, As(V) was 100% adsorbed on goethite below pH 7, though gibbsite maintained a measurable As(V) solution concentration.

The one-site CCM curves in Fig. 2 (lines) were fit to the two As(V) concentrations on each oxide using the optimization subroutine in FITEQL. The model provided reasonable qualitative descriptions of the experimental data on both goethite and gibbsite despite some overpredictions of As(V) adsorption on goethite between pH 7 and 9. The model also consistently overpredicted As(V) adsorption on gibbsite by approximately 4 mg kg^{-1} at the 133 µ*M* As(V) starting concentration (Fig. 2b). The one-site, monodentate-only assumption has been the conventional approach taken for surface complexation mod-

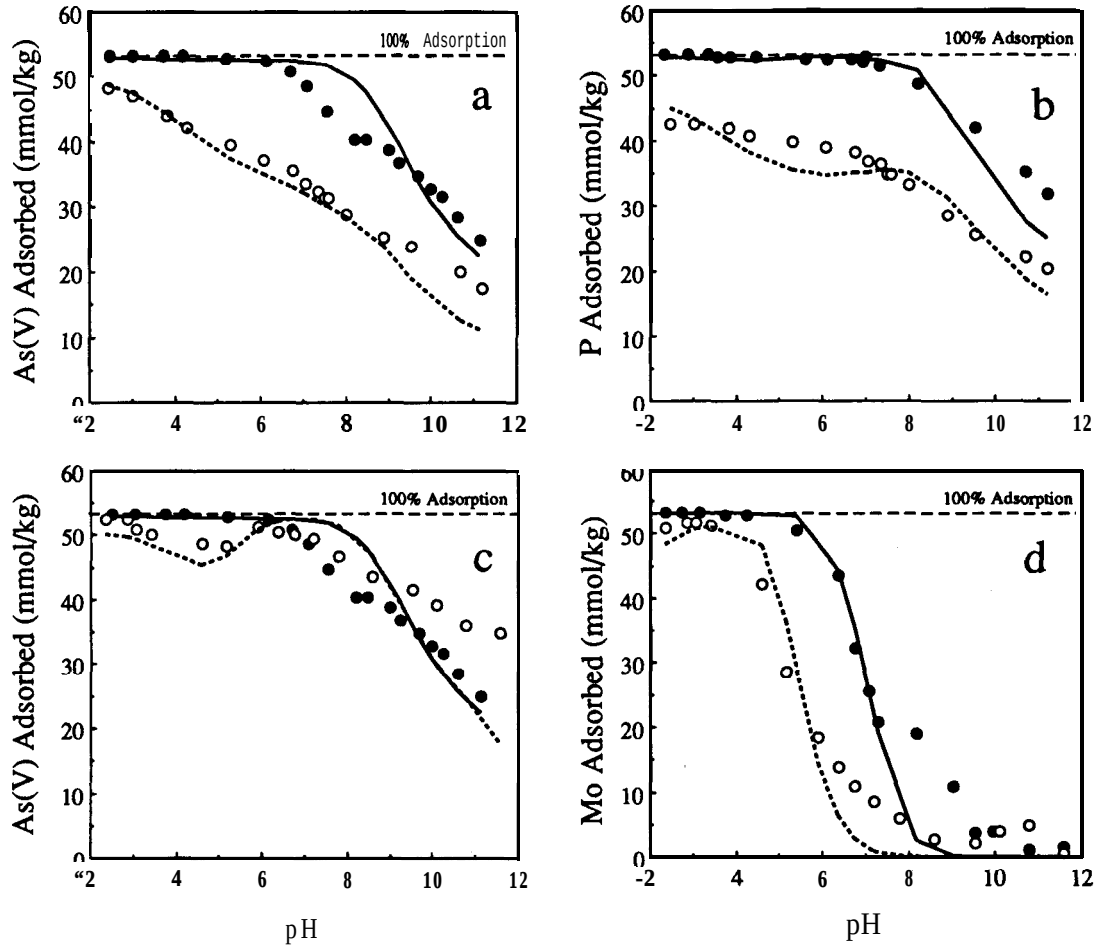

Fig. 3. Arsenate (a and c), phosphate (h), and molybdate (d) single-anion and binary anion adsorption envelopes on goethite **(α-FeOOH)** with constant capacitance model calculations using the one-site assumption. In all panels, symbols are: experimental single-anion data (filled circles), binary anion data (open circles), single-anion model calculations (solid lines), and binary anion model calculations (dotted tines). Reaction conditions: 133 μM As(V), P, or Mo (single-anion), 133 μM As(V) + 133 μM P or Mo (binary), 0.1 M NaCl, 2.5 g L^{-1} **α-FeOOH,** reaction time = 4 h, T = 23°C.

eling of As(V) adsorption on Fe and Al oxides (Goldberg, 1986) and sediments (Belzile and Tessier, 1990).

Single and binary anion experimental data and CCM lines using the one-site assumption are shown in Fig. 3. Both As(V) and P single anions displayed broad adsorption envelopes (filled circles, Fig. 3a and 3b) with 100% adsorption of As(V) below pH 6 and 100% adsorption of P below pH 7. These results were consistent with As(V) adsorption envelopes reported on hydrous Fe oxide (Hsia et al., 1994) and goethite (Hingston et al., 1971). The experimental As(V) and P adsorption envelopes on goethite in the binary As(V)/P systems (open circles, Fig. 3a and 3b) suggested that As(V) and P compete for adsorption sites on the goethite surface.

Molybdate adsorption on goethite (filled circles, Fig. 3d) displayed a stronger pH dependence than As(V) or P, with zero adsorption above pH 10 and a steep adsorption edge resulting in 100% Mo adsorption (53.2 mmol Mo kg-') below pH 5. Arsenate competitive adsorption caused a shift in the Mo adsorption edge (measured at 50% adsorption, or 26.5 mmol Mo kg^{-1}) from pH 7.4 to 5.4 (open circles, Fig. 3d) but did not change the overall shape of the Mo adsorption envelope. The presence of 133 μM Mo (open circles, Fig. 3c) altered the As(V) adsorption envelope by increasing As(V) adsorption above pH 7 while decreasing As(V) adsorption below pH 5.

The K_{Anion}**(int)** values for the As(V), P, and Mo single-anion systems (Table 1) were used to predict experimental adsorption envelopes in the binary systems. In Fig. 3, binary model predictions (dotted lines) agree with binary adsorption data (open circles) in most cases. Exceptions include the underprediction of P adsorption in the presence of As(V) on goethite at pH 4 to 7 (Fig. 3b) and the unexplainable increase in As(V) adsorption in the presence of Mo above pH 7 (Fig. 3c).

The experimental As(V) single-anion adsorption envelope for gibbsite showed a minimum in adsorption at pH 11.0, increasing at a rate of 8 mmol As(V) kg-' per pH unit decrease until an adsorption maximum was reached at pH 6.0 (Fig. 4a). The decrease in As(V) adsorption due to competition with P at pH 7 (15 mmol kg^{-1}) was the same for goethite and gibbsite. Arsenate decreased P adsorption on gibbsite by 8 mmol kg-' at pH 7 (Fig. 4b), indicating that gibbsite adsorbed P preferentially over As(V). The single Mo anion adsorp-

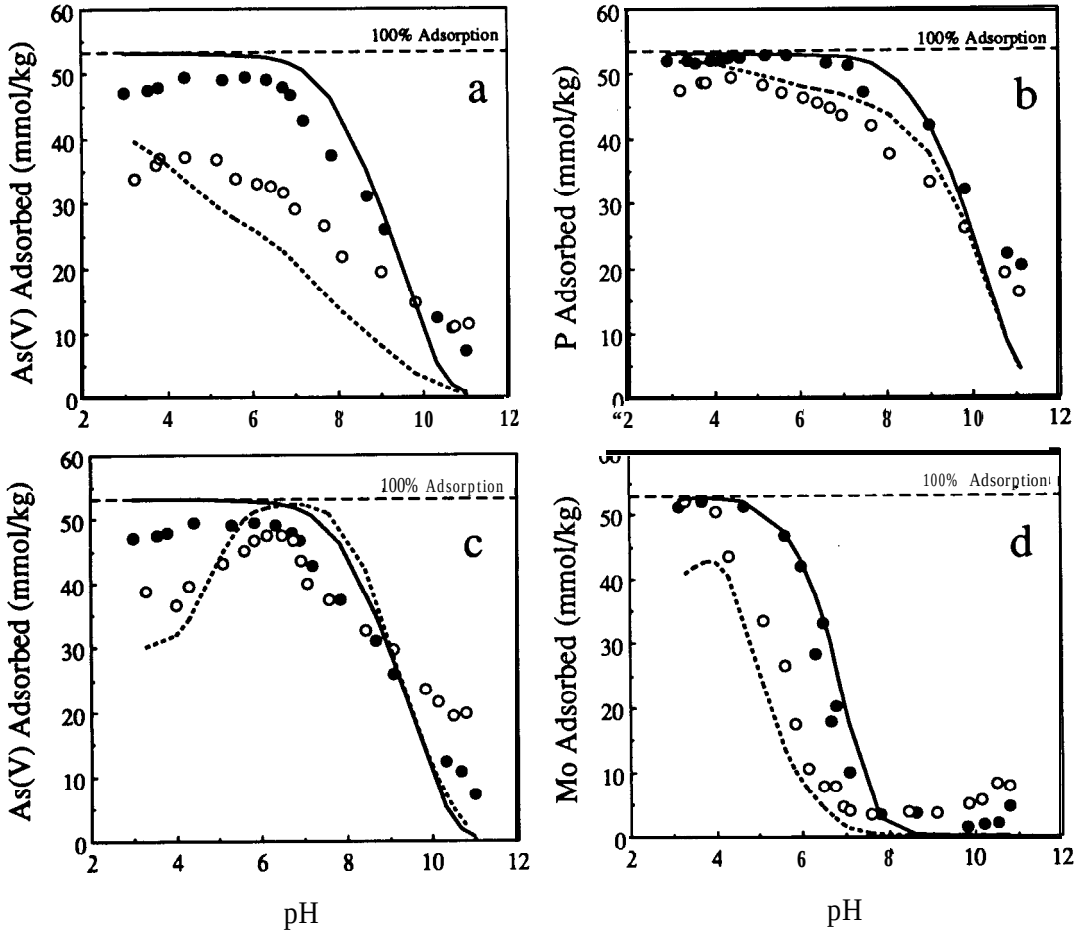

Fig. 4. Arsenate (a and c), phosphate (b), and molybdate (d) single-anion and binary anion adsorption envelopes on gibbsite [γ-Al(OH)$_3$] with constant capacitance model calculations using the one-site (SOH) assumption. In all panels, symbols are: experimental single-anion data (filled circles), binary anion data (open circles), single-anion model calculations (solid lines), and binary anion model calculations (dotted lines). Reaction conditions: 133 μM As(V), P, or Mo (single-anion), 133 μM As(V) + 133 μM P or Mo (binary), 0.1 M NaCl, 2.5 g L^{-1} γ-Al(OH)$_3$, reaction time = 4 h, T = 23°C.

tion envelope on gibbsite (filled circles, Fig. 4d) was similar in shape to that on goethite, but was slightly steeper, with sharper pH dependence. Arsenate adsorption on gibbsite was not substantially affected by the presence of equimolar Mo above pH 6 (Fig. 4c). Unlike goethite, however, As(V) adsorption on gibbsite was decreased by 10 mmol kg^{-1} (about 20%) due to competition with Mo at pH 4. Arsenate competition with Mo displaced the Mo adsorption edge (at 50% adsorption) 1.3 pH units from pH 6.9 to 5.6 (Fig. 4d). Greater than 95% of Mo was adsorbed below pH 4.0 in single Mo anion and binary As(V)/Mo anion systems on both goethite and gibbsite. These data suggest that As(V) occupies a fraction of the pH-dependent Mo adsorption sites on both goethite and gibbsite, and that another distinct fraction of sites has a higher affinity for Mo than As(V) at low pH.

Adsorption of polyprotic acids such as H_3AsO_4 and H_3PO_4 results in broad adsorption envelopes across a wide pH range (Sigg and Stumm, 1981), whereas the diprotic H_2MoO_4 species exhibits a steeper adsorption envelope. Adsorption of weak acids is strongest at pH values near the acid dissociation constants (pK_a) of the acid (Hingston et al., 1972). The two pK_a values for H_2MoO_4 (pK_{a1} = 4.00, pK_{a2} = 4.24; Lindsay, 1979) are in the pH region where preferential adsorption of Mo over As(V) was observed on the gibbsite surface.

The CCM predictions of competitive As(V) and P adsorption on gibbsite using the one-site assumption (dotted lines, Fig. 4a and 4b) were in poorer agreement with experimental data than on goethite. The model consistently underpredicted As(V) adsorption in the presence of P by an average of 10 mmol As(V) kg^{-1} between pH 4 and 10 (Fig. 4a). In this case the model successfully predicted that P would be preferentially adsorbed over As(V) on gibbsite, though it underpredicted the total co-adsorption of As(V) and P. Phosphate adsorption on gibbsite was slightly overpredicted by the model in the As(V)/P system below pH 10 (Fig. 4b).

The model was able to account for the mutual effects of As(V) and Mo on each other in the binary As(V)/Mo system (Fig. 4c and 4d). As with goethite, As(V) adsorption on gibbsite did not decrease due to the presence of equimolar Mo above pH 7, but was depressed as Mo loading increased below pH 5. In this case the model qualitatively described both the decrease in As(V)

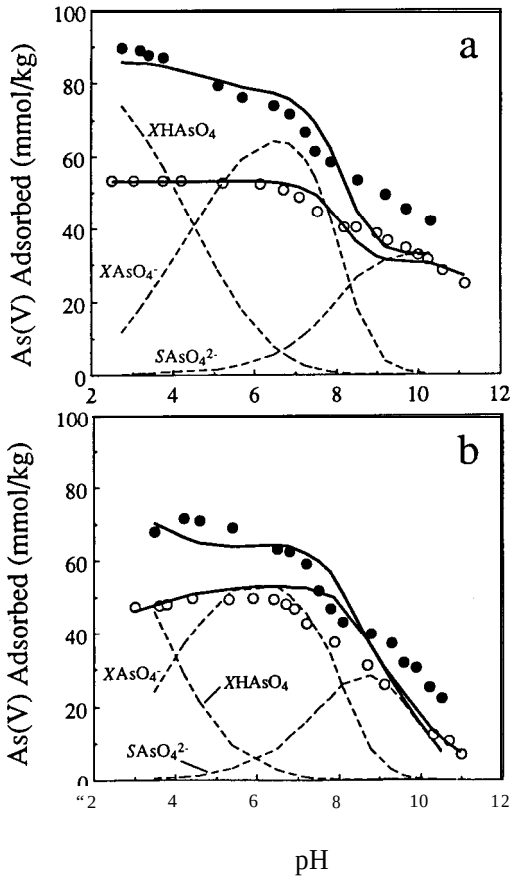

Fig. 5. Arsenate adsorption envelopes on goethite (α-FeOOH) (a) and gibbsite [γ-Al(OH)$_3$] (b) at two As(V) loadings showing constant capacitance model calculations using the two-site [SOH + $X(OH)_2$] assumption. Solid lines represent the sum of As(V) surface species as calculated by the model. Dotted lines correspond to individual As(V) surface species in the two-site model [266 μ*M* As(V)] only. Reaction conditions: 266 μ*M* As(V) (tilled circles) or 133 μ*M* As(V) (open circles), 0.1 M NaCl, 2.5 g L^{-1} solid, reaction time = 4 h, *T* = 23°C.

adsorption and the shift to lower pH of the Mo adsorption edge.

Two-Site Adsorption Modeling

Application of the two-site (monodentate + bidentate) model assumptions to experimental adsorption data at two As(V) concentrations resulted in reasonable agreement below pH 8 (Fig. 5). Figure 5 also includes the pH dependence of the predicted mono- and bidentate speciation ($XHAsO_4$, $XAsO_4^{2-}$, and $SAsO_4^{2-}$) in the 266 μ*M* As(V) system (dotted lines). It was assumed that bidentate As(V) complexes may also form on Al octahedra and thus gibbsite was treated in the same manner as goethite (Fig. 5b). It was desirable for the two-site model output for As(V) adsorption on goethite to be in approximate agreement with the proportions of mono- and bidentate As(V) coverage on ferrihydrite based on the EXAFS spectra (Waychunas et al., 1993). Hence, in this approach, a priori knowledge of surface speciation was used as a constraint in applying the model. Unfortunately, the present approach using the two-site, three-species ($XHAsO_4$, $XAsO_4^{2-}$, and $SAsO_4^{2-}$) assumptions is limited by the lack of detailed, quantitative information about the effects of changing pH on the protonation status of As(V), P, and Mo surface complexes.

The general shapes of the two-site model envelopes for both oxides did not agree with the experimental As(V) data, though the model gave reasonable representations below pH 8 for goethite (Fig. 5a). The model underpredicted As(V) adsorption on goethite in the 266 μ*M* As(V) system above pH 8 by 15 mmol kg^{-1}. As with the one-site constants, the two-site $K_{As(V)}$(int) values were sufficiently robust to describe As(V) surface coverages resulting from two As(V) starting concentrations. Model fits could be improved on both oxides by increasing the absolute values of $K_{S\pm}$(int) for the monodentate site, causing the $SAsO_4^{2-}$ species to adsorb at higher pH; however, the resulting PZC values for the SOH site based on Eq. [21] would have been unreasonably high. The final values of $K_{S\pm}$(int) used for the monodentate site (see Table 2) resulted in calculated PZC values for the SOH site of 12.0 and 11.5 for goethite and gibbsite, respectively.

The two-site model assumptions were applied to the entire data set, using single-anion K_{Anion}(int) values for As(V), P, and Mo (Table 2) to predict competitive adsorption behavior in binary anion systems (Fig. 6). Predictions of adsorbed As(V) and P on goethite in the binary As(V)/P system (dotted lines, Fig. 6a and 6b) agreed with experimental data below pH 8. Divergence from the experimental data above pH 8 was due to the decline of the $XAsO_4^{2-}$ species at higher pH (Fig. 5), a result of the restrictions placed on the amount of monodentate $SAsO_4^{2-}$ species adsorption due to strong evidence for the formation of predominantly bidentate surface complexes on Fe(III) oxides at pH 8 (Waychunas et al., 1993). The two-site model approach overpredicted the competitive effects of Mo on As(V) below pH 6 (dotted lines, Fig. 6c) and, as with the one-site approach, was able to describe the shift to lower pH in the Mo adsorption envelope due to As(V) competition (Fig. 6d).

The two-site model applied to As(V) competitive adsorption on gibbsite was generally not in agreement with the experimental data (Fig. 7a and 7c). This may be due to errors associated with using assumptions about the nature of As(V) surface complexes on Fe(III) oxides in modeling As(V) surface complexation on gibbsite. The lack of spectroscopic information concerning the identity of As(V) (or P and Mo) surface complexes on gibbsite may invalidate some of our model assumptions. Phosphate (Fig. 7b) and Mo (Fig. 7d) adsorption were more closely described by the two-site model than As(V), however predicted decreases in P and Mo adsorption due to competition with As(V) were slightly larger than the experimental data.

Previous efforts to model systems of competing anions have either been predictions using surface complexation constants optimized in binary anion systems containing different anion concentrations (Goldberg, 1986) or system-specific direct optimization of intrinsic equilibrium constants using the binary adsorption data (Goldberg and Traina, 1987). The ability of the CCM to predict co-adsorption of two competing anions in binary systems based on surface complexation constants optimized with

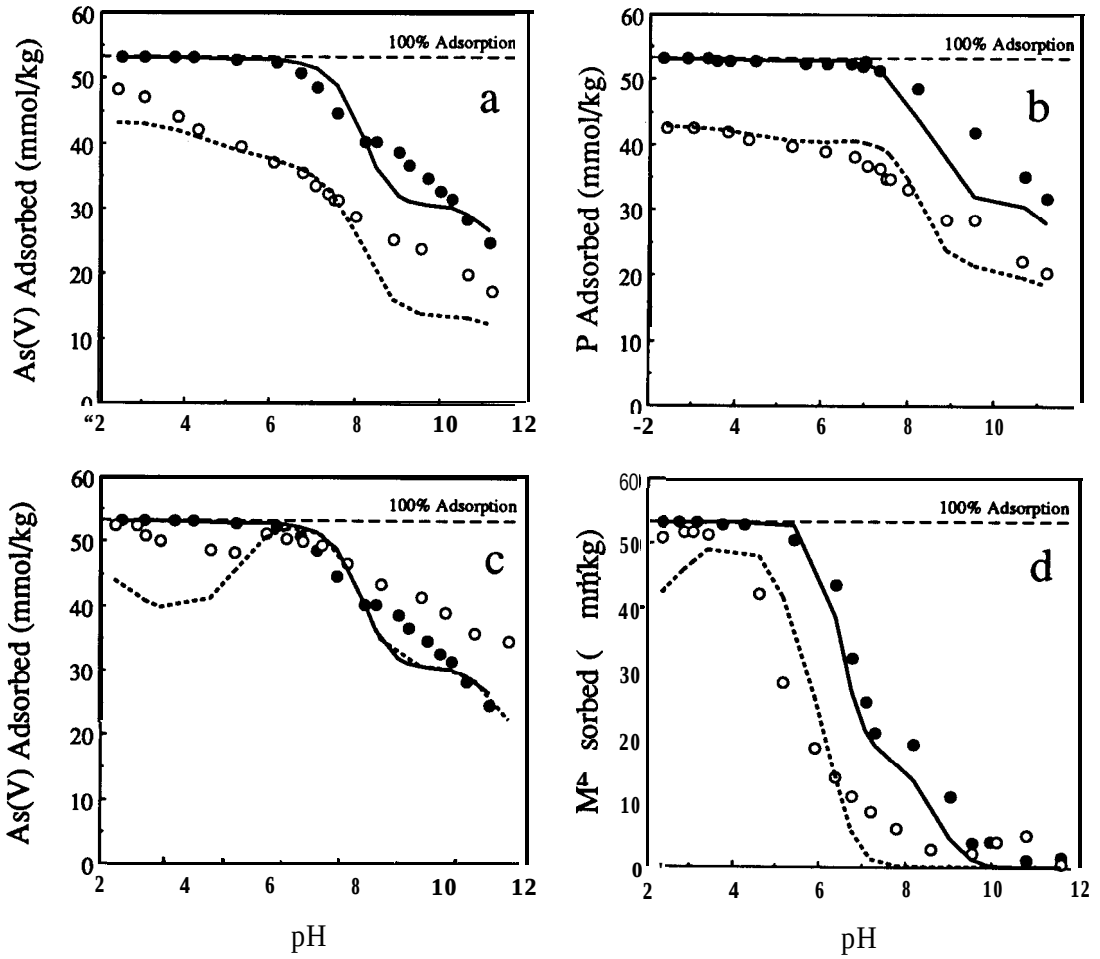

Fig. 6. Arsenate (a and c), phosphate (b), and molybdate (d) single-anion and binary anion adsorption envelopes on goethite (α-FeOOH) with constant capacitance model calculations using the two-site [SOH + $X(OH)_2$] assumption. In all panels, symbols are: experimental single-anion data (filled circles), binary anion data (open circles), single-anion model calculations (solid lines), and binary anion model calculations (dotted lines). Reaction conditions: 133 μ*M* As(V), P, or Mo (sin&-anion), 133 μ*M* As(V) + 133 μ*M* P or Mo (binary), 0.1 M NaCl, 2.5 g L^{-1} a-FeOOH, reaction time = 4 h, *T* = 23°C.

single-anion data represents an advancement in adsorption modeling of experimental data. In addition, previous work on surface complexation modeling of As(V) (Goldberg, 1986), P (Goldberg and Sposito, 1984; Goldberg and Traina, 1987; Bleam et al., 1991), and Mo (Zhang and Sparks, 1989; Motta and Miranda, 1989) considered only monodentate surface complexes. Sigg and Stumm (1981) considered both mono- and bidentate P surface complexes at a single site (SOH) on goethite, which gave excellent descriptions of experimental data, though surface speciation was assumed to be predominantly monodentate attachment. Our results suggest that surface complexation modeling may have applications in predicting competitive adsorption in more complex systems containing multiple competing ions.

CONCLUSION

In experimental adsorption envelopes, the relative affinity of As(V), P, and Mo for the goethite and gibbsite surfaces was pH dependent and tended to be P ≈ As(V) > Mo at neutral pH. Phosphate and As(V) appeared to compete for a similar set of surface sites, though there was evidence that some sites were uniquely available for adsorption of either As(V) or P. Site-specific behavior may be apparent in the binary As(V)/Mo systems as well, as indicated by a reversal in the relative affinity of the two anions at low pH.

The CCM adequately described experimental anion adsorption envelopes on goethite and gibbsite and was useful in providing a modeling framework in which to test assumptions regarding the mechanism of anion adsorption. Both the one-site and two-site modeling approaches used in this study gave similar fits of the CCM to experimental data. The nonuniqueness of these results suggests that our present understanding of anion adsorption on mineral surfaces is not complete. More detailed experimental information regarding anion adsorption at the oxide-water interface is required for unique model representations of the phenomenon including: (i) the effects of pH on the protonation status of adsorbed species and the partitioning between mono- and bidentate surface complexes, (ii) accurate and reproducible determinations of reactive surface site density of various minerals, and (iii) direct spectroscopic data on the adsorption mecha-

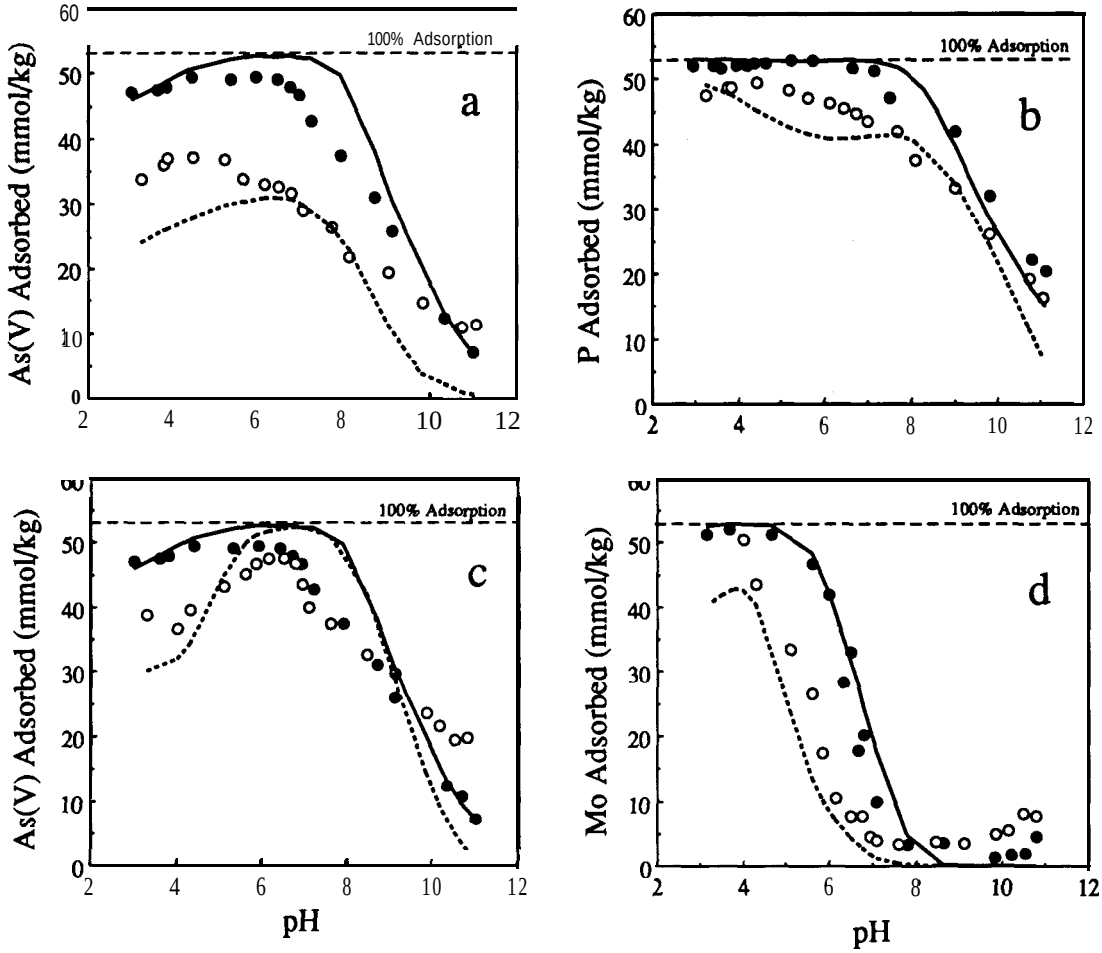

Fig. 7. Arsenate (a and c), phosphate (b), and molybdate (d) single-anion and binary anion adsorption envelopes on gibbsite [γ-Al(OH)$_3$] with constant capacitance model calculations using the two-site [SOH + X(OH)$_2$] assumption. In all panels, symbols are: experimental single-anion data (filled circles), binary anion data (open circles), single-anion model calculations (solid lines), and binary anion model calculations (dotted lines). Reaction conditions: 133 μM As(V), P, or Mo (single ion), 133 μM As(V) + 133 μM P or Mo (binary), 0.1 M NaCl, 2.5 g L^{-1} γ-Al(OH)$_3$, reaction time = 4 h, T = 23°C.

nisms of several ions on different materials. Successful simulation of the interactions of competing adsorbates in model systems of soil minerals will enhance our understanding of the mobility of environmental contaminants such as As(V) in whole soils.

ACKNOWLEDGMENTS

We gratefully acknowledge Harold Forster for the preparation of synthetic gibbsite and Dr. Dean Martens for assistance with ion chromatography.

REFERENCES

Anderson, M.A., and D. T. Malotky. 1979. The adsorption of protolyzable anions on hydrous oxides at the isoelectric pH. J. Colloid Interface Sci. 72:413-427.

Barrow, NJ. 1974. On the displacement of adsorbed anions from soil: 2. Displacement of phosphate by arsenate, Soil Sci. 117:28-33.

Belzile, N., and A. Tessier. 1990. Interactions between arsenic and iron oxyhydroxides in lacustrine sediments. Geochim. Cosmochim. Acta 54: 103-109.

Bleam, W .F., P.E. Pfeffer, S. Goldberg, R. W. Taylor, and R. Dudley. 1991. A ^{31}P solid-state nuclear magnetic resonance study of phosphate adsorption at the boehmite/aqueous solution interface. Langmuir 7:1702-1712.

Cotton, F.A., and G. Wilkinson. 1980. Advancedinorganic chemistry. 4th ed. Wiley-Interscience, New York.

Davis, J.A., and D.B. Kent. 1990. Surface complexation modeling in aqueous geochemistry. Rev. Mineral. 23:177-260.

Dzombak, D.A., and F.M.M. Morel. 1990. Surface complexation modeling. Hydrous ferric oxide. Wiley-Interscience, New York.

Ferreiro, E.A., A.K. Helmy, and S.G. de Bussetti. 1985. Molybdate sorption by oxides of aluminum and iron. Z. Pflanzenernaehr. Bodenkd. 148:559-566.

Fuller, C.C., J.A. Davis, and G.A. Waychunas. 1993. Surface chemistry of ferrihydrite: Part 2. Kinetics of arsenate adsorption and coprecipitation. Geochim. Cosmochim. Acta 57:2271-2282.

Goldberg, S. 1986. Chemical modeling of arsenate adsorption on aluminum and iron oxide minerals. Soil Sci. Soc. Am. J. 50: 1154-1157.

Goldberg, S. 1995. Adsorption models incorporated into chemical equilibrium models. p. 75-95. In R.H. Loeppert et al. (ed.) Chemical equilibrium and reaction models. SSSA Spec. Publ. 42. ASA and SSSA, Madison, WI.

Goldberg, S., H.S. Forster, and E.L. Heick. 1993. Boron adsorption mechanisms on oxides, clay minerals, and soils inferred from ionic strength effects. Soil Sci. Soc. Am. J. 57:704-708.

Goldberg, S., and R.A. Glaubig. 1988. Anion sorption on a calcareous, montmorillonitic soil – Arsenic. Soil Sci. Soc. Am. J. 52: 1297-1300.

Goldberg, S., and G. Sposito. 1984. A chemical model of phosphate adsorption by soils: I. Reference oxide minerals. Soil Sci. Soc. Am. J. 48:772-778.

Goldberg, S., and S.J. Traina. 1987. Chemical modeling of anion competition on oxides using the constant capacitance model – Mixed-ligand approach. Soil Sci. Soc. Am. J. 51:929-932.

Harrison, J.B., and V.E. Berkheiser. 1982. Anion interactions with freshly prepared hydrous iron oxides. Clays Clay Miner. 30:97-102.

Herbelin, A.L., and J.C. Westall. 1994. FITEQL: A computer program for the determination of chemical equilibrium constants from experimental data. Version 3.1. Rep. 94-01. Oregon State Univ., Corvallis.

Hingston, F.J. 1981. A review of anion adsorption. p. 51-90. In M.A. Anderson and A.J. Rubin (ed.) Adsorption of inorganics at solid-liquid interfaces. Ann Arbor Sci. Publ., Am Arbor, MI.

Hingston, F.J., A.M. Posner, and J.P. Quirk. 1971. Competitive adsorption of negatively charged ligands on oxide surfaces. Discuss. Faraday Soc. 52:334-342.

Hingston, F.J., A.M. Posner, and J.P. Quirk. 1972. Anionadsorption by goethite and gibbsite. I. The role of the proton in determining adsorption envelones. J. Soil Sci. 23:177-192.

Hohl, H., L. Sigg, and W. Stumm. 1980. Characterization of surface chemical properties of oxides in natural waters. Adv. Chem. Ser. 189:1-31.

Hohl, H., and W. Stumm. 1976. Interaction of Pb^{2+} with hydrous γ-Al_2O_3. J. Colloid Interface Sci. 55:281-288.

Hsia, T.H., S.L. Lo, C.F. Lin, and D.Y. Lee. 1994. Characterization of arsenate adsorption on hydrous iron oxide using chemical and physical methods. Colloids Surf. A: Physicochem. Eng. Aspects 85: l-7.

Hunter, R.J. 1981. Zeta potential in colloid science. Principles and applications. Academic Press, London.

Jacobs, L.W., J.K. Syers, and D.R. Keeney. 1970. Arsenic sorption by soils. Soil Sci. Soc. Am. J. 34:750-754.

Kvle. J.H.. A.M. Posner. and J.P. Ouirk. 1975. Kinetics of isotopic *exchange of phosphate adsorbed on gibbsite. J. Soil Sci. 26:32-43.

Leckie, J.O., M.M. Benjamin, K. Hayes, G. Kaufman, and S. Altmann. 1980. Adsorption/coprecipitation of trace elements from water with iron oxyhydroxide. Final Rep. EPRI CS-1513. Electric Power Res. Inst., Palo Alto, CA.

Lindsay, W.L. 1979. Chemical equilibria in soils. Wiley-Interscience, New York.

Livesey, N.T., and P.M. Huang. 1981. Adsorption of arsenate by soils and its relation to selected chemical properties and anions. Soil Sci. 131:88-94.

Lumsdon, D.G., and L.J. Evans. 1994. Surface complexation model parameters for goethite (a-FeOOH). J. Colloid Interface Sci. 164: 119-125.

Lumsdon, D.G., A.R. Fraser, J.D. Russell, and N.T. Livesey. 1984. New infrared band assignments for the arsenate ion adsorbed on synthetic goethite (α-FeOOH). J. Soil Sci. 35:381-386.

Masscheleyn, P.H., R.D. Delaune, and W.H. Patrick. 1991. Effect of redox potential and pH on arsenic speciation and solubility in a contaminated soil. Environ. Sci. Technol. 25:1414-1419.

McLaughlin, J.R., J.C. Ryden, and J.K. Syers. 1981. Sorption of inorganic phosphate by iron and aluminum-containing components. J. Soil Sci. 32:365-377.

Motta, M.M., and C.F. Miranda. 1989. Molybdate adsorption on kaolinite, montmorillonite, and illite: Constant capacitance modeling. Soil Sci. Soc. Am. J. 53:380-385.

Murali, V., and L.A.G. Aylmore. 1983. Competitive adsorption during solute transport in soils: 3. A review of experimental evidence of competitive adsorption and an evaluation of simple competition models. Soil Sci. 136:279-290.

Pierce, M.L., and C.B. Moore. 1982. Adsorption of arsenite and arsenate on amorphous iron oxyhydroxide. Water Res. 16: 1247-1253.

Roy, W.R., J.J. Hassett, and R.A. Griffin. 1986. Competitive coefficients for the adsorption of arsenate, molybdate, and phosphate mixtures by soils. Soil Sci. Soc. Am. J. 50:ll76-1182:

Sadia. M.. T.H. Zaida, andA.A. Mian. 1983. Enviromnentalbehavior of-arsenic in soils:. Theoretical. Water Air Soil Pollut. 20:369-377.

Schindler, P.W., B. Fürst, R. Dick, and P.U. Wolf. 1976. Ligand properties of surface silanol groups. I. Surface complex formation with Fe'+, Cu^{2+}, Cd*+, and Pb^{2+}. J. Colloid Interface Sci. 55: 469-475.

Schindler. P.W.. and H. Gamsjäger. 1972. Acid-base reactions of the TiO_2 (anatase)-water interface and the point of zero charge of TiO, suspensions. Kolloid Z. Z. Polvm. 250:759-763.

Sigg, L., and W. Stumm. 1981. The interactions of anions and weak acids with the hydrous goethite (α-FeOOH) surface. Colloids Surf. 2:101-107.

Stumm, W., H. Hohl, and F. Dalang. 1976. Interactions of metal ions with hydrous oxide surfaces. Croat. Chem. Acta 48:491-504.

Stumm, W., R. Kummert, and L. Sigg. 1980. A ligand exchange model for the adsorption of inorganic and organic ligands at hydrous oxide interfaces. Croat. Chem. Acta 53:291-312.

Waychunas, G.A., B.A. Rea, C.C. Fuller, and J.A. Davis. 1993. Surface chemistry of ferrihvdrite: Part 1. EXAFS studies of the geometry of coprecipitated and adsorbed arsenate. Geochim. Cosmochim. Acta 57:2251-2269.

Westall, J.C. 1982. FITEQL: A computer program for determination of equilibrium constants from experimental data. Rep. 82-01. Dep. of Chem., Oregon State Univ., Corvallis.

Westall, J.C., and H. Hohl. 1980. A comparison of electrostatic models for the oxide/solution interface. Adv. Colloid Interface Sci. 12:265-294.

Zhang, P.C., and D.L. Sparks. 1989. Kinetics and mechanims of molybdate adsorption/desorption at the goethite/water interface using pressure-jump relaxation. Soil Sci. Soc. Am. J. 53: 1028-1034.